

SIRIUS: A Code on Fission Product Behavior under Severe Accident

Kwang Soon Ha*, Sung Il Kim, Hyung Seok Kang, and Dong Ha Kim
Korea Atomic Energy Research Institute, 1045 Daedeok-daero, Yuseong-gu, Daejeon, Korea
*Corresponding author: tomo@kaeri.re.kr

1. Introduction

The major threat of nuclear power plants to the safety of the public comes from the radioactive materials present in the reactor vessel. The amount of radionuclides released into the containment or to the environment is always the focus of the design, operation, and regulation of a nuclear power plant. In particular, a large amount of radioactive materials might be released if a core melt accident, that is, a severe accident, occurs in a nuclear power plant. Therefore, it is very important to estimate the behaviors of radioactive materials under severe accident conditions.

The transport phases of the radioactive materials can be divided into gas and aerosol. The gas and aerosol phases of the radioactive materials move through the reactor coolant systems and containments as loaded on the carrier gas or liquid, such as steam or water. Most radioactive materials might escape in the form of aerosols from a nuclear power plant during a severe reactor accident [1], and it is very important to predict the behavior of these radioactive aerosols in the reactor cooling system and in the containment building under severe accident conditions. Aerosols are designated as very small solid particles or liquid droplets suspended in a gas phase. The suspended solid or liquid particles typically have a range of sizes of 0.01 to 20 μm . Aerosol concentrations in reactor accident analyses are typically less than 100 g/m^3 and usually less than 1 g/m^3 . At these concentrations, the aerosol particles have little effect on the gas hydrodynamics, but the gas dynamics profoundly affect the behavior of the suspended particles. The behaviors of the larger aerosol particles are usually described through continuum mechanics. The smallest particles have diameters of less than the mean free path of the gas phase molecules, and the behavior of these particles can often be described well through free molecular physics. The vast majority of aerosol particles arising in reactor accident analyses have behaviors in the very complicated intermediate regime between the continuum mechanics and free molecular limit. In this regime, the aerosol behavior must be described using an approximate solution to the Boltzmann equation [1]. When there are continuing sources of aerosol to the gas phase or when there are complicated processes involving engineered safety features, much more complicated size distributions

develop. It is not uncommon for aerosols in the reactor containments to have bimodal size distributions for at least some significant periods of time early during an accident. Salient features of aerosol physics under reactor accident conditions that will affect the nature of the aerosols are (1) the formation of aerosol particles, (2) growth of aerosol particles, (3) shape of aerosol particles, (4) deposition of particles on the surfaces, and (5) a re-suspension of aerosol particles [1].

At KAERI, a SIRIUS (Simulation of Radioactive nuclides Interaction Under Severe accidents) code has been developed to predict the behaviors of the radioactive materials in the reactor coolant system and in the containment under severe accident conditions. SIRIUS consists of an estimation of the initial inventories, species release from the core, aerosol generation, gas transport, and aerosol transport. The final outcomes of the SIRIUS designate the radioactive gas and aerosol distribution in the reactor coolant system and in the containment.

2. Descriptions of SIRIUS

As shown in Fig. 1, SIRIUS consists of an estimation of the initial inventories, species release from the core, aerosol generation, gas transport, and aerosol transport.

In the fission product module, the initial inventories of the fission species in UO_2 such as Xe, Kr, Cs, I, Te, Sb, Se, Ba, Sr, Ru, Mo, and La Zr (fission) are calculated based on SANDIA-ORIGEN calculation data [2], which are a function of the reactor thermal power and the fuel cycle or OPR1000-ORIGEN calculation data [3]. SANDIA-ORIGEN calculation data were obtained by assuming a 3412 MWt Westinghouse PWR, end-of-cycle equilibrium core, and three-region core, each initially loaded with fuel enriched to 3.3% U-235, with a constant specific power density of 38.3 MW per metric ton of U, a three-year refueling cycle, an 80% capacity factor, and three regions having burn-ups of 11,000, 22,000, and 33,000 MWd per metric ton of uranium [2]. OPR1000-ORIGEN calculation data were obtained by one assembly calculation for Uljin unit 6 of an OPR 1000 type using the ORIGEN code [3].

The other inventories that come from the structure materials, such as Zr, Fe, Cr, Ni, and Mn, are calculated from the masses of the cladding, stainless steel, and Inconel alloy.

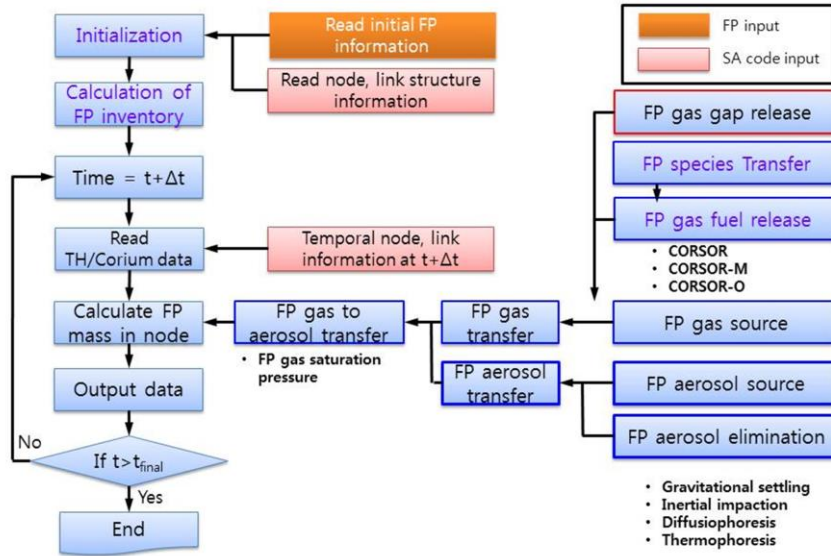


Fig. 1. Structure of fission product module

Radioactive and nonradioactive species may be released from the core, cladding, structural materials such as stainless steel, and Inconel alloy if the materials heat up. The species release rates are calculated using the CORSOR, CORSOR-M, and CORSOR-O models [2], which is a function of the material temperature. The released species are eight classified groups that have similar chemical properties, that is, noble gases, alkali metal iodides, alkali metal hydroxides, chalcogens, alkaline earths, platinoids, rare earths, and structural materials, as shown in Table I. It is assumed that the released species from the core, cladding, and structural materials are initially formed as representative groups of the gas phases. Each group has its own saturation gas pressure according to the temperature. Therefore, some amount of aerosols of each group may be generated if the gas pressure is higher than the saturation pressure, and some aerosols of each group may be evaporated into gas if the gas pressure is lower than the saturation pressure. The saturation pressure of group 1, noble gases, is zero, and therefore the noble gases cannot form aerosols.

The gases and aerosols of fission products are transported through the reactor coolant systems and containments as loaded into the carrier gas or liquid such as steam or water. If the reactor coolant systems and containments are nodalized and linked by a general thermal-hydraulic code, the fission product transport equations for the gas and aerosol phases of the i -group can be designated using equations (1) and (2) at the given thermal-hydraulic node n .

$$\frac{dm_{v,i}^n}{dt} = \dot{m}_{v,i,in}^n - \dot{m}_{v,i,out}^n + \hat{G}_{v,i}^n \quad (1)$$

$$\frac{dm_{a,i}^n}{dt} = \dot{m}_{a,i,in}^n - \dot{m}_{a,i,out}^n - \lambda_{t,i}^n m_{a,i}^n + \hat{G}_{a,i}^n \quad (2)$$

Table I: Fission Product Groups

Group	Representative	Species member
1. Noble gases	Xe	Xe, Kr
2. Alkali metal iodides	CsI	CsI
3. Alkali metal hydroxides	CsOH	CsOH
4. Chalcogens	Te	Te, Sb, Se
5. Alkaline earths	Ba	Ba, Sr
6. Platinoids	Ru	Ru, Mo
7. Rare earths	La	La, Zr(fission)
8. Structural materials	Zr	Zr, Fe, Cr, Ni, Mn

The i -group gas generation rate in a node n , $\hat{G}_{v,i}^n$, in equation (1) can be obtained by the CORSOR, CORSOR-M, CORSOR-O, and gap releasing models [2] or user input data. The i -group aerosol generation rate in node n , $\hat{G}_{a,i}^n$, in equation (2) can be obtained by the user input. The i -group gas and aerosol mass flow rates in node n are estimated using the mass transport rates of the carrier gas or liquid, which are calculated by the thermal-hydraulic module in the severe accident codes. Therefore, the fission product model should be coupled with the thermal-hydraulic module. In equation (2), the i -group aerosol removal coefficient in a node n , $\lambda_{t,i}^n$, can be obtained by considering the aerosol behaviors such

as the gravitational settling, thermophoresis, impaction, diffusiophoresis (steam condensation), vapor condensation, and vapor revolatilization. There are several approaches to predict the aerosol dynamics such as a sectional method [2, 4] and mass tracking method [5, 6, 7, 8]. Based on the mass tracking method similar to the MAAP 5 code [8], some aerosol behaviors such as the gravitational settling [5], impaction [5], diffusiophoresis [6], and thermophoresis [7] are considered to estimate the aerosol removal coefficient. The gas and aerosol transport equations in equations (1) and (2) are discretized to apply semi-implicit (Gauss-Jordan elimination) or explicit (Runge-Kutta-Fehlberg, RK45) numerical schemes for time marching.

After solving the *i*-group gas and aerosol transport equations, the *i*-group gas and aerosol masses are re-evaluated using the saturation pressure of the *i*-group gas according to the temperature, as mentioned before.

SIRIUS was prepared using C++ language. A user can select a semi-implicit or explicit numerical scheme for solving the gas and aerosol transport equations, and add user-defined gas and aerosol groups, which include the properties and source rates.

3. Results and Discussion

The individual modules of the SIRIUS code, such as calculation modules for the initial inventory, decay heat, aerosol generation, sedimentation, impaction, thermophoresis, diffusiophoresis, and wall deposition, have been verified by simulating various virtual problems and experiments.

The aerosol generation module was validated using a virtual problem, as shown in Fig. 2. The carrier gas was assumed as having two different paths, and the temperatures in the nodes were changed. Fig. 3 shows the airborne CSI aerosol masses in node 4 and node 8. As shown in Fig. 3, the CsI aerosol in node 8 is higher than in node 4, that is, the aerosols are generated in node 8 much more, because node 8 is cooled down.

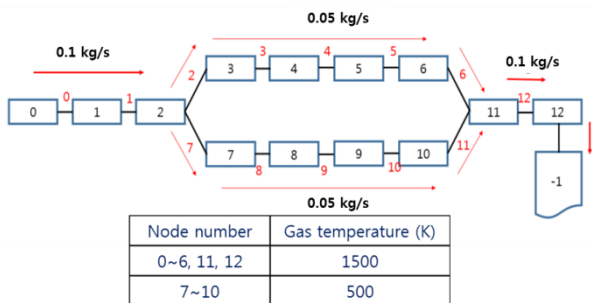


Fig. 2. Problem definition for verifying aerosol generation module

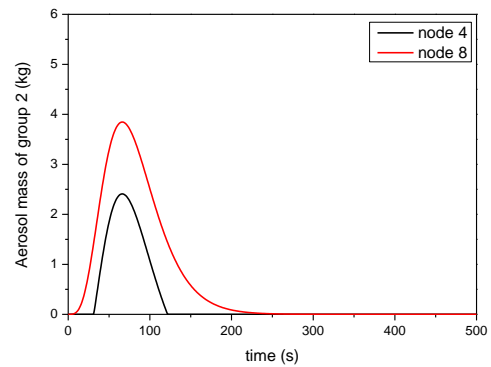


Fig. 3. Airborne CsI aerosol mass in nodes 4 and 8

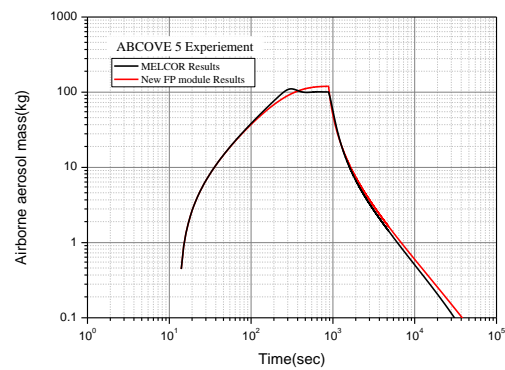


Fig. 4. Temporal variation of airborne aerosol mass compared with MELCOR results on AB-5 experiment

The aerosol coagulation and removal models in the developed fission product module were verified through a comparison with the MELCOR results in the ABCOVE (AB-5, AB-6, AB-7) and LACE (LA2) experiments [9]. In all calculations, thermal-hydraulic data obtained by the MELCOR calculations were used to calculate the airborne mass by the fission product module. User-defined aerosol groups in each calculation were created to match with the experimental conditions. Only the aerosol sedimentation model during each calculation was activated in the fission product module. As shown in Fig. 4, the temporal airborne sodium aerosol mass by the SIRIUS code agreed excellently with the MELCOR results.

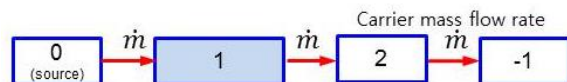


Fig. 5. Problem definition for verifying aerosol elimination modules

Table II: Calculation results for aerosol impaction

Case name		IMP-0	IMP-1	IMP-2	IMP-3	IMP-4	IMP-5
Node 0 Aerosol injection	Injection time (sec)	0-300	0-300	0-300	0-300	0-300	0-300
	Injection rate (kg/sec)	1	1	1	1	1	1
Node 2 Impaction grating	Node area (m ²)	0.1	0.1	0.1	0.1	0.001	0.1
	Impaction diameter (m)	0	0.0001	0.01	0.0001	0.0001	0.0001
	Impaction area (m ²)	0	100	100	10	100	100
Link information	Mass flow rate (\dot{m})	1	1	1	1	1	10
Steady state Results	Airborne mass in Node 0 (kg)	1	1	1	1	1	0.1
	Airborne mass in Node 1 (kg)	1	0.997519	0.99978	0.999935	0.517735	0.0996831
	Impaction efficiency (%)	0	0.2481	0.022	0.0065	48.2265	0.3169

Table III: Calculation results for aerosol thermophoresis

Case name		TPS-1	TSP-2	TSP-3	TSP-4	TSP-5	TSP-6
Node 0 Aerosol injection	Injection time(s)	0-100	0-100	0-100	0-100	0-100	0-100
	Injection rate (kg/s)	1	1	1	1	1	1
Node 1	Flow area (m ²)	0.1	0.1	0.1	0.1	0.1	0.1
	Wall temperature (K)	400	500	600	700	800	900
	Wall area (m ²)	10	10	10	10	10	10
Link info.	Mass flow rate (\dot{m})	1	1	1	1	1	1
Steady state Results	Airborne mass in Node 0 (kg)	1	1	1	1	1	1
	Airborne mass in Node 1 (kg)	0.91933	0.94473	0.96246	0.97554	0.98558	0.99354
	Thermophoresis efficiency (%)	8.067	5.527	3.754	2.446	1.442	0.646

Table IV: Calculation results for aerosol diffusiophoresis

Case name		DPS-0	DPS-1	DPS-2	DPS-3	DPS-4	DPS-5
Node 0 Aerosol Injection	Injection time(s)	0-100	0-100	0-100	0-100	0-100	0-100
	Injection rate(kg/s)	1	1	1	1	1	1
Node 2	Total pressure (bar)	10	10	10	10	10	10
	Steam pressure (bar)	1	3	5	7	9	9
	Steam temperature (K)	374	407	425	438	449	448.5
	Wall temperature (K)	372	405	423	436	447	448.5
Link Info.	Mass flow rate (\dot{m})	1	1	1	1	1	1
Steady State Results	Airborne mass in Node 0 (kg)	1	1	1	1	1	1
	Airborne mass in Node 1 (kg)	0.99865	0.99072	0.97512	0.94208	0.85843	1
	Diffusiophoresis efficiency (%)	0.135	0.928	2.488	5.792	14.257	0.0

Fig. 5 shows a virtual problem definition for validation of aerosol elimination modules such as aerosol impaction, thermophoresis, and diffusiophoresis. In Fig. 5, the aerosol source is imposed in node 0, and aerosol eliminations by impaction, thermophoresis, and diffusiophoresis occurs only in node 1.

In Table II, aerosol impaction efficiencies are summarized according to the impaction diameter and area. As shown in Table II, aerosol impaction efficiency

increases as the impaction diameter decreases and the impaction area increases.

In Table III, aerosol elimination efficiencies by thermophoresis are summarized according to the wall temperature. As shown in Table III, aerosol elimination efficiencies by thermophoresis increases as the wall temperature decreases.

In Table IV, aerosol elimination efficiencies by diffusiophoresis are summarized according to the steam pressure. As shown in Table IV, aerosol elimination

efficiencies by diffusiophoresis increases as the wall temperature increases.

3. Conclusion

A SIRIUS (Simulation of Radioactive nuclides Interaction Under Severe accidents) code was developed to predict the behaviors of the radioactive materials in a reactor coolant system and in the containment under severe accident conditions. SIRIUS consists of an estimation of the initial inventories, species release from the core, aerosol generation, gas transport, and aerosol transport. The individual modules of the SIRIUS code, such as calculation modules for aerosol generation, sedimentation, impaction, thermophoresis, diffusiophoresis, and wall deposition, have been verified by simulating various virtual problems and an ABCOVE experiment.

SIRIUS will be updated by adding some models related to the aerosol size tracking, aerosol elimination in the pool, iodine behaviors in the gas and pool, etc. In addition, the SIRIUS code may be used as a fission product module of the CINEMA code to analyze the severe accident phenomena in a nuclear power plant.

NOMENCLATURE

$m_{v,i}^n$	i -group gas mass in n node
$\dot{m}_{v,i,in}^n$	i -group gas mass inflow rate into n node
$\dot{m}_{v,i,out}^n$	i -group gas mass outflow rate from n node
$\dot{G}_{v,i}^n$	i -group gas mass source rate in n node
$m_{a,i}^n$	i -group aerosol mass in n node
$\dot{m}_{a,i,in}^n$	i -group aerosol mass inflow rate into n node
$\dot{m}_{a,i,out}^n$	i -group aerosol mass outflow rate from n node
$\dot{G}_{a,i}^n$	i -group aerosol mass source rate in n node
$\lambda_{t,i}^n$	i -group aerosol removal coefficient in n node

ACKNOWLEDGMENTS

This work was supported by the Nuclear and Development of the Korea Institute of Energy Technology Evaluation and Planning (KETEP) grant funded by the Korea government (Ministry of Trade, Industry, and Energy) (No. 20141510101670).

REFERENCES

[1] State-of-the-art report on nuclear aerosols, NEA/CSNI/ R(2009)5, Nuclear Energy Agency, Committee on the safety of nuclear installations, Dec. 17, 2009.

[2] R.O. Gauntt, R.K. Cole, C.M. Erickson, R.G. Gido, R.D. Gasser, S.B. Rodriguez, and M.F. Young, MELCOR Computer Code Manual, Vol. 2: Reference Manuals, Version 1.8.5 May 2000, Decay Heat(DCH) Package Manual, RadioNuclide(RN) Package

Reference Manual, NUREG/CR-6119, Vol. 2, Rev. 2, SAND2000-2417/2, October 2000.

[3] Eun Hyun Ryu, Hae Sun Jeong, Dong Ha Kim, Comparison of the Results of the Whole Core Decay Power Using the ORIGEN Code and ANS-1979 for the Uljin Unit 6, Transactions of the Korean Nuclear Society Spring Meeting, Jeju, Korea, May 7-8, 2015.

[4] F. Gelbard, MAEROS User Manual, SAND80-0822, NUREG/CR-1391, December 1982.

[5] Michael Epstein and Phillip G. Ellison, "Correlations of the rate of removal of coagulating and depositing aerosols for application to nuclear reactor safety problems," NED, 107, p. 327-344, 1988.

[6] R. T. Lahey and F. J. Moody, The thermal-hydraulics of a boiling water nuclear reactor. 2nd ed., ANS, La Grange Park, 1993.

[7] Michael Epstein and Phillip G. Ellison, "Thermophoretic deposition of particles in nature convection flow from a vertical plate," J. Heat Transfer, Vol. 107, p.272-276, 1985

[8] MAAP5 Code Manual

[9] Francisco J. Souto, F. Eric Haskin, Lubomyra N. Kmetyk, MELCOR 1.8.2 assessment: aerosol experiments ABOVE AB5, AB6, AB7, and LACE LA2, SAND-2166, SNL. 1994.